TREATMENT

EFFECT OF COOLING RATE ON THE STRUCTURE OF LOW-CARBON LOW-ALLOY STEEL AFTER THERMOMECHANICAL CONTROLLED PROCESSING

M. L. Lobanov,[1] M. L. Krasnov,[2] V. N. Urtsev,[3] S. V. Danilov,[1] and V. I. Pastukhov[1, 4]

The method of orientation microscopy (EBSD) is used to study the structure and texture of low-carbon low-alloy pipe steel after thermomechanical controlled processing (TMCP) and subsequent quenching at cooling rates 100 – 700 K/sec.

Key words: pipe steels, thermomechanical controlled processing (TMCP), bainite, martensite, orientation microscopy, texture, orientation relations, special boundaries.

INTRODUCTION

Cross-country large-diameter pipes for transporting gas and oil are produced from sheets fabricated from high-strength low-carbon low-alloy steels [1, 2]. An obvious advantage of the use of high-strength pipes is reduced metal intensity (wall thickness) [1, 3]. A breakthrough improvement of the structural strength of low-alloy pipe steels occurred in the middle 1970s due to the development and integration of thermomechanical controlled processing (TMCP), which combines controlled rolling and subsequent controlled accelerated cooling [3 – 7]. It should be noted that commercial application of TMCP in Russia reached a new level after installation of special rolling mills 5000 by the "Severstal'" (Kolpino), "VMZ" (Vyksa) and "MMK" (Magnitogorsk) Companies.

Transfer from steels of strength classes X52 – X65 to X70 – X80 (K60 – K65) and to X100 (~ K80) corresponded to transition from ferrite-pearlite microstructures to structures with dominance of products of shear transformation (primarily bainite) formed due to controlling the stability of supercooled austenite by alloying and application of accelerated cooling [2, 4, 7 – 10].

The new level of production of articles with specified functional properties and predictable structures requires control of the parameters of the production processes in accordance with the kinetics of the physical properties occurring in the material [9 – 13].

The aim of the present work was to study the laws of structure formation in low-carbon low-alloy steel under continuous cooling accompanied by a $\gamma \rightarrow \alpha$ shear transformation.

METHODS OF STUDY

Various rates of cooling of samples including those matching the parameters of commercial production were simulated in an original bench designed at the "Ausferr" RTC and consisting of a heating furnace with a mechanism for withdrawal and fixation of samples, a unit for temperature measurement, a unit for air cooling with a pneumatic system, and a unit for control and recording the information [14].

We studied samples cut from a commercial sheet of a low-carbon low-alloy steel of type 06G2MB (about 0.05% C, $\leq$ 2.0% Mn, about 0.2% Mo, about 0.05% Nb, the remainder Fe and inevitable impurities) used for making large-diameter pipes of strength class K60, K65. The sam-

---

[1] Ural Federal University after the First President of Russia B. N. Eltsyn, Ekaterinburg, Russia (e-mail: m.l.lobanov@urfu.ru).
[2] Magnitogorsk Iron and Steel Works (MMK), Magnitogorsk, Russia.
[3] "Ausferr" RTC, Magnitogorsk, Russia.
[4] Institute of Reactor Materials, Zarechny, Sverdlovsk Oblast, Russia.

TABLE 1. Thermophysical and Structural Parameters for Various Cooling Modes of Samples from Steel 06G2MB

Mode	$dT/d\tau$, K/sec	t_{0tr}, °C	t_{tr}, °C	τ_{tr}, sec	Q_{tr}, kJ/kg	D_m, μm	X_m/D_m
1	693	~ 680	~ 400	~ 1.0	~ 31	0.97 ± 0.03	2.19
2	449	692	494	2.0	113	1.2 ± 0.1	2.15
3	202	671	367	4.8	118	1.5 ± 0.1	2.07
4	166	662	337	6.6	114	1.7 ± 0.1	2.00
5	110	673	366	8.6	108	1.8 ± 0.1	1.90

ples had the form of plates 20×70 mm in size, the thickness of which was varied from 0.25 to 1.10 mm. Such sizes of the samples provided a heat exchange in one preferred direction under heating and cooling.

The samples were heated in the bench furnace to the austenitization temperature of 980°C (without dissolution of carbide phases (chiefly NbC) precipitated under the industrial TMCP) and held for 30 min. The rate of cooling of the samples was controlled by their thickness and by the pressure in the air cooling system. After some tests, we obtained a set of samples cooled in the temperature range from 980°C to the effective temperature of the start of phase transformations t_{0tr} at a rate $(dT/d\tau)$ in the range of $100 - 700$ K/sec (see Table 1 and Fig. 1). The experimentally obtained thermograms were also used to determine the effective temperatures t_{tr} of the end of the phase transformations, the time intervals of their implementation τ_{tr}, and the heat effects Q_{tr}.

The samples were used to prepare metallographic specimens in the ND – RD plane (where RD is the rolling direction in the TMCP and ND is the direction normal to the rolling plane) for studying the microstructure and the texture.

The electron microscope study of the structure was performed using a Tescan Mira3 scanning microscope with an autoelectronic cathode at an accelerating voltage of 20 kV. To determine the orientation of individual grains and to analyze local textures, we used an EBSD HKL Inca attachment with an Oxford Instruments system for analysis. The scanning step was 0.1 μm. The error in the determination of the orientation of the crystal lattice was at most $\pm 1°$ ($\pm 0.6°$ on the average). The low-angle boundaries between local volumes were plotted on the orientation maps at misorientations from 1 to 6° (lines with a thickness of 1 pixel); at misorientations of at least 15° we plotted high-angle boundaries (lines with a thickness of 3 pixels). In the range of $7 - 15°$, we also plotted low-angle boundaries but with a somewhat greater thickness (lines with a thickness of 2 pixels).

The high accuracy of the identification of the orientations, and hence of the local misorientations in the EBSD analysis (over 95% recognition for all the domains studied), allowed us to use the Oxford Instruments software for determining the parameters of the microstructure of the specimens, i.e., the mean size of the crystallites (D_m) and their elongation over the ND (X_m/D_m) (see Table 1). The size D_m was determined as the diameter of a circle equivalent to the
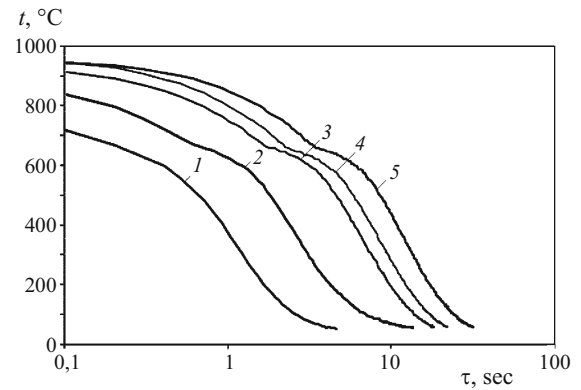

Fig. 1. Variation of the temperature of samples from steel 06G2MB as a function of the time at various cooling rates: *1*) $v_{cool} = 693$ K/sec; *2*) 449 K/sec; *3*) 202 K/sec; *4*) 166 K/sec; *5*) 110 K/sec.

mean area of the crystallites. A crystallite was an object singled out on all the sides by boundaries with misorientation angles of at least 7°.

The special boundaries between individual grains were analyzed by plotting them on the orientation maps with allowance for the standard Brandon criterion $\pm\Delta\Theta$ employed in the software. This criterion has a specific value for each boundary, i.e., $\Delta\Theta = 15°/(\Sigma n)^{1/2}$, where Σn is the number of coinciding sites under superimposition of three-dimensional crystal lattices. The texture was studied by plotting the distribution functions of the misorientations (DFM).

Analyzing the orientations, we used a coordinate system, the axes of which were correlated to the hot rolling direction in the TMCP ($X \parallel$ RD), to the normal to its plane ($Y \parallel$ ND), and to the perpendicular direction ($Z \parallel$ PD) coinciding with the axis of the rolls, so that the three axes formed a right-hand triple of vectors.

RESULTS AND DISCUSSION

The microstructure and the texture of steel 06G2MB after cooling from the austenitic range at various rates are presented in Fig. 2.

After cooling at a high rate ($v_{cool} = 693$ K/sec) the specimens had a lath structure typical for martensite and repre-
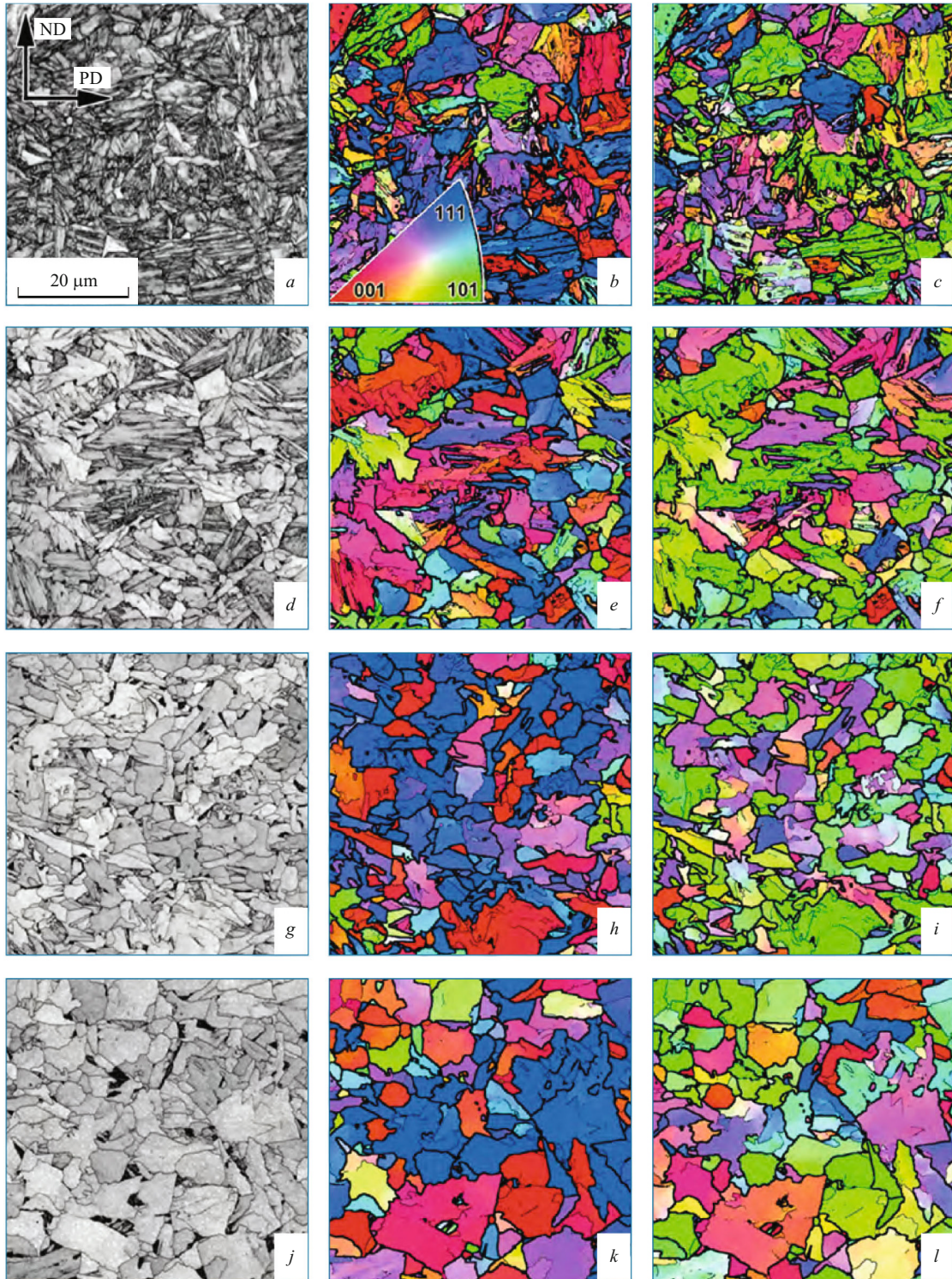
Fig. 2. Microstructure and texture of steel 06G2MB in the form of orientation maps (EBSD) after cooling from the austenitic range at various rates (the stereographic triangle with color differentiation of the crystallographic orientations is given in Fig. 2*b*): *a, b, c*) v_{cool} = 693 K/sec; *d, e, f*) 449 K/sec; *g, h, i*) 202 K/sec; *j, k, l*) 110 K/sec; *a, d, g, j*) orientation contrast (BC); *b, e, h, k*) colored maps with ND; *c, f, i, l*) colored maps with RD.

sented by alternating plates with a thickness from 0.5 to 2 μm and a length of up to 10 μm (Fig. 2*a*). We observed 2 – 3 crystallographic directions of the crystallites within one

martensite lath (Fig. 2*b* and *c*). Lowering of vcool to 449 K/sec caused formation of a much less homogeneous structure in which the martensite laths were accompanied by

comparatively large individual (outside the laths) crystallites with nonequilibrium shapes (Fig. 2d – f) and a maximum size of about 20 μm.

At the cooling rates of 202 and 166 K/sec martensite laths were virtually absent. The structure was represented by not equiaxed crystallites with irregular geometry and maximum size of up to 20 μm with small "dark" inclusions on their boundaries (Fig. 2g – i). It could be seen at a high magnification that these inclusions were inhomogeneous precipitates and had an own substructure resembling a lath one.

Further decrease of the cooling rate to 110 K/sec and a lower temperature made the crystallites of the main structure more equiaxed (Fig. 2j – l). The boundaries of the crystallites tended to be "straightened." The volume fraction and the sizes of the "dark" inclusions increased. The orientation microscopy (Fig. 2k and l) allows us to classify these inclusions as martensite laths, where the carbon-enriched austenite decomposed in the last turn.

The observed variation of the sizes and shapes of large crystallites formed at $v_{cool} = 449$ K/sec and lower cooling rates in the section corresponding to the plane of the lap allows us to assume that most of them should be shaped as lens- or disc-like plates in a three-dimensional space.

When the samples were cooled at a rate of 693 K/sec, the spectra of the intercrystallite boundaries corresponded to a martensitic structure (Fig. 3a – c) [15, 16]. All the high-angle boundaries were concentrated within misorientation angles from 49 to 60° (Fig. 3b). The spectra of the special boundaries corresponded to only CSL-boundaries, i.e., Σ3, Σ11, Σ25b, Σ33c, and Σ41c. It has been shown in [15] that the appearance of this spectrum is a result of a shear phase transformation according to the orientation relations (OR) intermediate between the Kurdyumov–Sachs (K-S) OR and Nishiyama–Wasserman (N-W) OR.

Lowering of the cooling rate to 449 K/sec, which causes appearance of coarse out-of-lath crystallites in the structure, did not affect substantially the spectra of the intercrystallite boundaries (Fig. 3d – f). At a lower cooling rate causing formation of more "equilibrium" structures with "dark" inclusions, we observed a comparatively little number of high-angle boundaries with misorientation angles from 35 to 48° (Fig. 3h). In the spectra of the CSL-boundaries (Fig. 3g and i) we observed appearance of special boundaries, the most manifested of which were Σ7, Σ9, Σ17b, Σ29b, Σ31b, Σ33a, Σ39b, Σ41c, Σ43c, and Σ45c. By the data of [17], the appearance of most of them is connected with implementation of relaxation processes (cell formation and start of primary recrystallization) in a bcc lattice.

It is interesting that the crystallographic textures of the samples cooled at substantially different rates and thus having different microstructures have turned out to be close enough (Fig. 4). In the first approximation, this texture may be considered as a set of α ((⟨110⟩ ∥ ND) and γ (⟨111⟩ ∥ RD) components. A more detailed analysis allows us to say that this texture has been formed by a set of limited components, i.e., (001)[1$\bar{1}$0] and couples from the families {113}⟨110⟩, {112}⟨110⟩, {111}⟨110⟩, {111}⟨112⟩. The intensity and the degree of scattering of the texture components could change at random noticeably depending on the place of imaging and was virtually uncorrelated to the cooling rate of the samples. It should be mentioned that this texture after a double phase recrystallization ($\alpha_B \to \gamma \to \alpha_M$ or $\alpha_M + \alpha_B$ or α_B) reproduces quite accurately the texture of a sheet with dominantly bainitic structure after the TMCP [12, 16].

Analysis of the crystallographic interdependence of the texture components of a bcc lattice after a heat treatment with supposedly earlier existing orientations of the γ-phase shows that all of them may be obtained in accordance with the orientations of the texture of the rolled austenite {112}⟨111⟩, {110}⟨111⟩, {110}⟨112⟩, {110}⟨001⟩ intermediate between the K-S OR and the N-W OR [18 – 21]. This matching stipulates implementation of kind of texture inheritance under phase transformations in the material. The main components of the texture of the austenite (stable orientations under deformation of the fcc lattice) transform into a discrete set of orientations of a bcc lattice under the TMCP [20, 21]. During subsequent heating, the orientations of the bcc lattice transform into an austenite texture coinciding with the texture of the γ-phase under the isothermal hot deformation during the TMCP. Hardening of the newly appearing austenite results in formation of structure by a shear phase transformation mechanism with the corresponding set of texture components of the bcc lattice [16].

The inheritance of texture observed in the samples after the TMCP implies the presence of components responsible for it [21], in our case the components "preserved" during processing of the material. By the data of [12, 16], these components are the special boundaries close to the CSL-boundaries Σ3 and, probably, Σ11 between the deformed austenite grains, which have formed under the hot rolling. The relative arrangement of these boundaries in the structure of the material is fixed additionally by precipitates of carbide phases.

The use of special boundaries as "carriers" of structure and texture inheritance seems to be justifiable. Only for such boundaries is it possible to describe their motion at the level of dislocation slip and climb. The presence and motion of special boundaries explains simply enough the formation and development of local textures in polycrystalline materials during structural transformations [22, 23]. It has been shown in [17] that formation of nuclei of a shear transformation is much easier on the boundaries of deformation and recrystallization twins, i.e., when nucleation occurs on the Σ3 special boundary. It should be stressed that according to theoretical computations and experimental observations the special boundaries Σ3 and Σ11 in a fcc lattice possess a minimum surface energy [23], i.e., may serve substrates for nuclei of a new phase or new grains [24]. It should also be noted that the
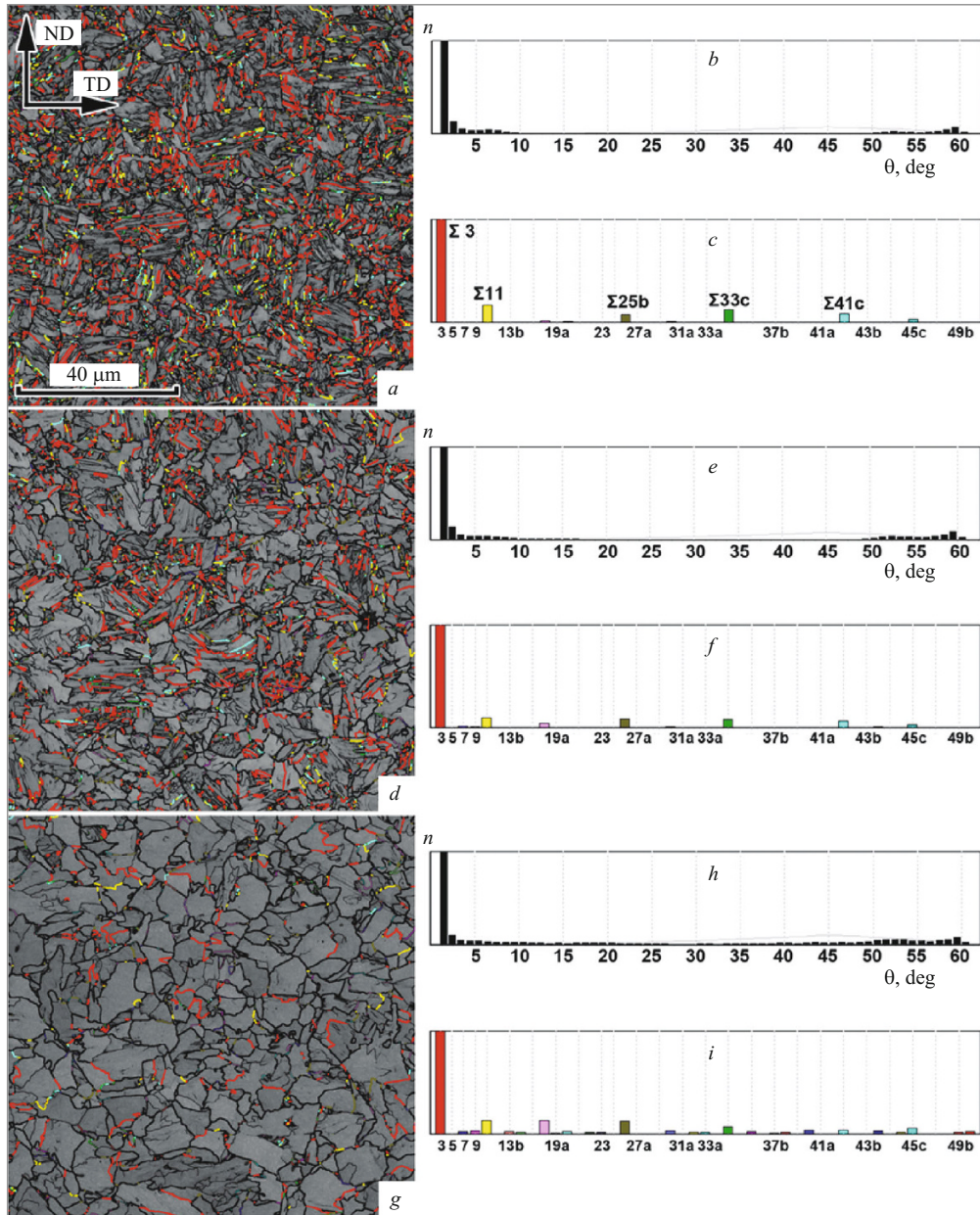
Fig. 3. Intercrystallite boundaries detected by orientation microscopy (EBSD) in the microstructure of specimens of steel 06G2MB cooled at various rates: *a, b, c*) $v_{cool} = 693$ K/sec; *d, e, f*) 449 K/sec; *g, h, i*) distribution of boundaries with respect to misorientation angles Θ; *c, f, i*) spectra of CSL-boundaries.

special boundaries near the temperature of phase transition may be sources of transformation dislocations.

It is obvious that within the approach described all the structures observed in the samples cooled at $v_{cool} < 449$ K/sec should be treated as largely ferritic ones. Note that the temperature of the thermodynamically equilibrium ("diffusion") $\gamma \to \alpha$ transformation (A_3) computed using the ThermoCalc software for the steel studied is about 820°C. According to the thermograms (Fig. 1), the effective temperatures of the start of phase transformations for all the cooling rates range within 670 – 700°C (see Table 1), i.e.,

match the range of diffusion transformation. A considerable part of the transformations occurs at 620 – 670°C, i.e., under conditions close to isothermal ones (Fig. 1). The time of the transformations at any v_{cool} is several seconds (see Table 1), which is typical of the shear transformation mechanism. The heat effect of the transformations computed from the thermograms is 110 – 120 kJ/kg (see Table 1) [14]. Its value is twice higher than the effect of the martensitic transformation for low-carbon steels [25].

It seems that the "behavior" of the transformation implemented in the steel at various cooling rates is mainly deter-
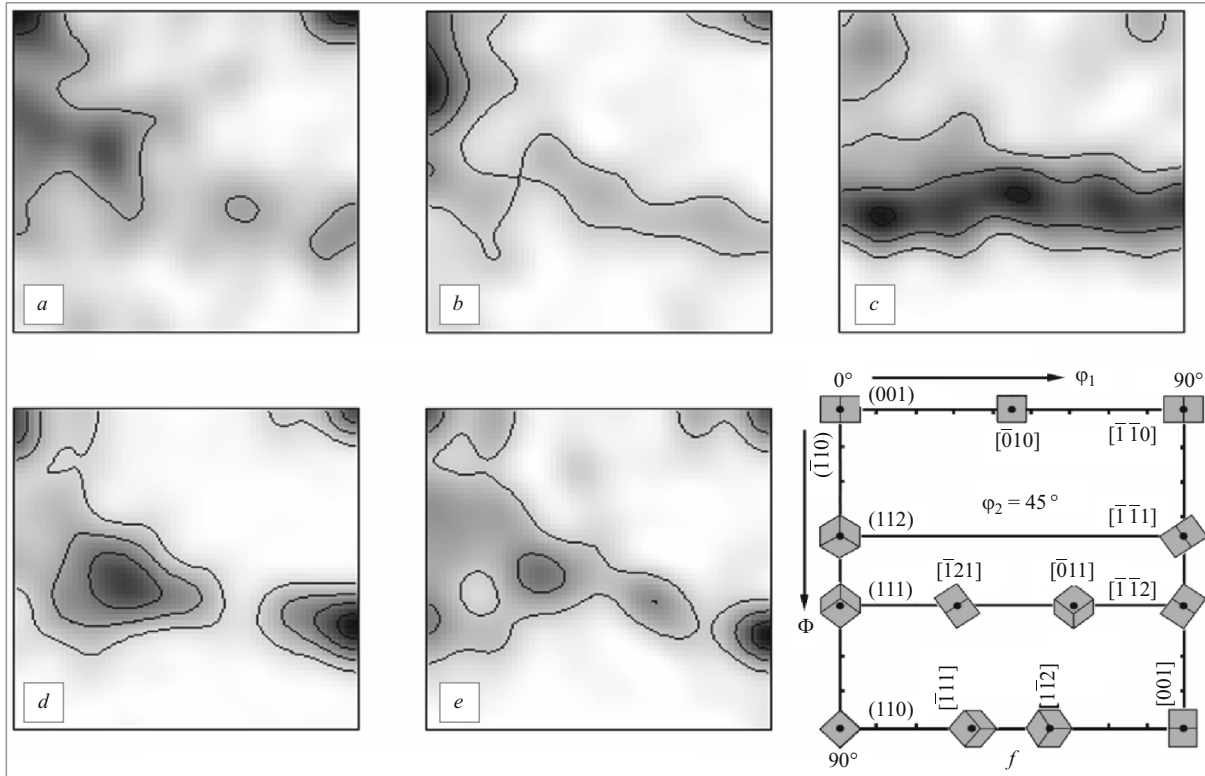
Fig. 4. Texture in the form of distribution functions of the orientations (EBSD) of samples of steel 06G2MB subjected to TMCP, after austenitization at 980°C and cooling at various rates (we present the sections of the space of Euler angles at $\varphi = 0°$ and $\varphi_2 = 45°$): *a*) $v_{cool} = 693$ K/sec; *b*) 449 K/sec; *c*) 202 K/sec; *d*) 166 K/sec; *e*) 110 K/sec; *f*) standard mesh for DFM at $\varphi = 0°$ and $\varphi_2 = 45°$ with deposited ideal orientations in the form of elementary crystallographic cells (viewed from ND).

mined by the time of metastable existence of the austenite, i.e., by the time of cooling from A_3 to t_{0tr} during which the carbon atoms are redistributed among local regions of the γ-phase. With allowance for the opinion that nuclei of the phase transformations (including "diffusion" ones) form on special boundaries, we may assume that in the case of a martensitic transformation carbon atoms are not redistributed substantially over the grain boundaries. The nuclei (or "substrates") for the shear phase transformation are small (matching the thickness of plates in the martensite laths) regions of high-angle boundaries having a structure close to a special (crystallographic) one. When the time of existence of the austenite in metastable condition is longer, the length of the segments of the boundaries with special structure increases substantially (at most to the distance between ternary junctions). Accordingly, any high-angle boundary becomes a potential source for one nucleus (one orientation) of a shear ("bainitic") or even ferritic ("diffusionless") phase transformation.

Thus, the results of the present work give us grounds to assume that the differences in the mechanisms of martensitic, bainitic and ferritic ("diffuionless") phase transformations in steels are mainly reduced to the size of the regions of special boundaries of type $\Sigma 3$, which are "activated" in the process of redistribution of carbon in the austenite.

CONCLUSIONS

1. An γ → α transformation in specimens of low-carbon low-alloy steel subjected to thermomechanical controlled processing with cooling rates of $100 - 450$ K/sec from the austenitic range starts at $700 - 670°$C and develops by a shear mechanism. The transformation yields a chiefly bainitic structure with inclusions of martensite regions. With growth of the cooling rate, the size of the bainite grains decreases, and the sizes and the volume fraction of the martensite inclusions increase.

2. The structure formed as a result of TMCP exhibits textural heredity after the subsequent heat treatment. The textural heredity manifests itself in the fact that a treatment involving double phase recrystallization $\alpha_{TMCP} \to \gamma \to \alpha_{HT}$ reproduces the TMCP texture. The carriers of the structural inheritance are special boundaries close to CSL-boundaries $\Sigma 3$ and $\Sigma 11$. The initial special boundaries form between stable orientations of the austenite grains in the process of hot rolling under the TMCP.

REFERENCES

1. K. Hulka, P. Peters, and F. Heisterkamp, "Tendencies in development of steels for large-size pipes," *Stal'*, No. 10, 62 – 67 (1997).
2. A. B. Arabey, "Requirements on the metal in gas pipelines," *Steel in Transl.*, **40**(7), 601 – 608 (2010).
3. D. J. Stalheim, "Recent schemes for alloying high-strength steels for cross-country oil-and-gas pipelines, Pt. 1," *Metallurg*, No. 11, 53 – 66 (2013).
4. E. Shigeru and N. Naoki, "Development of thermo-mechanical control process (TMCP) and high performance steel in JFE Steel," *JFE Techn. Rep.*, 20, 1 – 7 (2015).
5. Yu. D. Morozov, S. Yu. Nastich, M. Yu. Muratov, et al., "Obtaining high-quality properties of rolled material for large-diameter pipes based on formation of ferrite-bainite microstructure," *Metallurgist*, **52**(1 – 2), 21 – 28 (2008).
6. M. Yu. Matrosov, A. A. Kichkina, A. A. Efimov, et al., "Simulating structure-forming processes in tube steels during controlled rolling with accelerated cooling," *Metallurgist*, **51**(7 – 8), 367 – 376 (2007).
7. S. Yu. Nastich, Yu. D. Morozov, M. Yu. Matrosov, et al., "Assimilation of production in an MMK 500 mill of thick rolled sheet from low-alloy steels with improved strength and cold resistance properties," *Metallurgist*, **55**(11 – 12), 810 – 828 (2012).
8. S. Y. Nastich, V. L. Kornilov, Y. D. Morozov, et al., "New steels for pipelines of strength class K54 – K60 (X70): Production experience at OAO MMK," *Steel in Transl.*, **39**(5), 431 – 436 (2009).
9. H. K. Sung, S. Y. Shin, B. Hwang, et al., "Effects of carbon equivalent and cooling rate on tensile and Charpy impact properties of high-strength bainitic steels," *Mater. Sci. Eng. A*, **530**(1), 530 – 538 (2011).
10. Z. J. Xie, X. P. Ma, C. J. Shang, et al., "Nano-sized precipitation and properties of a low-carbon niobium micro-alloyed bainitic steel," *Mater. Sci. Eng. A*, **641**, 37 – 44 (2015).
11. E. A. Goli-Oglu, L. I. Efron, and Yu. D. Morozov, "Effect of deformation regime in main samples of controlled rolling on pipe steel microstructure," *Metal Sci. Heat Treat.*, **55**(5 – 6), 294 – 297 (2013).
12. I. Y. Pyshmintsev, A. O. Struin, A. M. Gervasyev, et al., "Effect of bainite crystallographic texture on failure of pipe steel sheets made by controlled thermomechanical treatment," *Metallurgist*, **60**(3 – 4), 405 – 412 (2016).
13. M.-C. Zhao, K. Yang, and Y. Shan, "The effects of thermo-mechanical control process on microstructures and mechanical properties of a commercial pipeline steel," *Metal Sci. Eng. A*, **335**(1 – 2), 14 – 20 (2002).
14. M. L. Lobanov, G. M. Rusakov, V. N. Urtsev, et al., "Thermal effect of bainitic transformation in tube steel by accelerated cooling," *Lett. Mater.*, **8**(2), 246 – 251 (2018).
15. M. L. Lobanov, G. M. Rusakov, A. A. Redikul'tsev, et al., "Investigation of special misorientations in lath martensite of low-carbon steel using the method of orientation microscopy," *Phys. Met. Metallogr.*, **117**(3), 254 – 259 (2016).
16. M. L. Lobanov, M. D. Borodina, S. V. Danilov, et al., "Texture inheritance on phase transition in low-carbon, low-alloy pipe steel after thermomechanical controlled processing," *Steel in Transl.*, **47**(11), 710 – 716 (2017).
17. G. M. Rusakov, M. L. Lobanov, A. A. Redikul'tsev, et al., "Special misorientations and textural heredity in the commercial alloy Fe – 3% Si," *Phys. Met. Metallogr.*, **115**(8), 775 – 785 (2014).
18. M. Holscher, D. Raabe, and K. Lucke, "Relationship between rolling textures and shear textures in f.c.c. and b.c.c. metals," *Acta Metall. Mater.*, **42**(3), 879 – 886 (1994).
19. L. Kestens and J. J. Jonas, "Transformation and recrystallization textures associated with steel processing," in: S. L. Semiatin (ed.), *Metalworking: Bulk Forming, ASM Handbook*, ASM International, Materials Park, Ohio, USA (2005), Vol. 14A, pp. 685 – 700.
20. B. Hutchinson, L. Ryde, E. Lindh, et al., "Texture in hot rolled austenite and resulting transformation products," *Mater. Sci. Eng. A*, **257**(1), 9 – 17 (1998).
21. T. Tomida and M. Wakita, "Transformation texture in hot-rolled steel sheets and its quantitative prediction," *ISIJ Int.*, **52**(4), 601 – 609 (2012).
22. N. Nakada, H. Ito, Y. Matsuoka, et al., "Deformation-induced martensitic transformation behavior in cold-rolled and cold-drawn type 316 stainless steels," *Acta Mater.*, **58**(3), 895 – 903 (2010).
23. F. J. Humphreys and M. Hatherly, *Recrystallization and Related Annealing Phenomena*, Elsevier Ltd, Oxford (2004), 574 p.
24. Yu. N. Gornostyrev, M. I. Katsnelson, A. R. Kuznetsov, and A. V. Trefilov, "Role of grain boundaries in heterogeneous nucleation of martensite phase," in: V. N. Urtsev (ed.), *Phase and Structural Transformations in Steels, Coll. Works* [in Russian], Magnitogorsk (2001), Issue 1, pp. 209 – 219.
25. H. K. D. H. Bhadeshia, "Martensite and bainite in steels: Transformation mechanism & mechanical properties," *J. De Physique IV*, **7**(5), C5-367 – C5-376 (1997).